Characteristics of a 128 × 128 liquid-crystal spatial light modulator for wave-front generation

Doo Jin Cho

Department of Physics, Ajou University, Suwon 442-749, Korea

Samuel T. Thurman, J. T. Donner, and G. Michael Morris

The Institute of Optics, University of Rochester, Rochester, New York 14627

Received February 9, 1998

Spatial and temporal characteristics of a 128 × 128 zero-twist nematic liquid-crystal spatial light modulator are investigated for wave-front generation at a wavelength of 632.8 nm. The modulator is found to have the capability of producing at least eight phase levels between 0 and 2π, and the rate of arbitrary phase modulation is limited to approximately 4.5 Hz. Wave-front generation of the first 55 Zernike polynomials is demonstrated. © 1998 Optical Society of America

OCIS codes: 010.1080, 160.3710, 230.6120, 010.7350.

Recently liquid-crystal spatial light modulators (LC SLM's) have been receiving much attention in various disciplines including adaptive optics (AO).[1] It has been demonstrated that LC SLM's can provide a convenient and effective means of amplitude or phase modulation or both. They have the advantages of low cost, high reliability, compactness, low power requirements, ease of controllability, and a potentially large number of correcting elements. Disadvantages of LC SLM's are that they have slow response times and generally require polarized light. Sixty-nine-element[2] and one hundred twenty-seven–element[3] LC SLM's, specifically designed for wave-front control, have been used to demonstrate the potential for AO applications. Dynamic performance of one of the 69-element devices was also investigated.[4] It is expected that a LC SLM will be a good replacement for the deformable mirror used in AO retinal imaging experiments.[5]

We characterize a zero-twist nematic LC SLM[6] for wave-front generation. The LC SLM, fabricated by Boulder Nonlinear Systems, Inc.,[7] has the capability of generating continuous phase modulation from 0 to 3π for polarized light at a wavelength of 632.8 nm. We demonstrate that it can produce high-quality wave fronts with its 128 × 128 pixel array. Features of the device include 40-μm pixel pitch, 5.12 mm × 5.12 mm array size, 60% fill factor, and 2-μm LC thickness. Sixteen 8-bit digital-to-analog converters load image frames to the device at approximately 9 kHz. The device is based on the electro-optic S effect, which requires true and inverse frames to be loaded alternately for each image.

Except in the research on temporal characterization, the LC SLM was evaluated with a Fizeau interferometer, as shown in Fig. 1. Linearly polarized light from a He–Ne laser was expanded by a beam expander, which consisted of a spatial filter and collimating lens, and then reflected off a reference surface and the LC SLM. When the polarization of the illuminating light is oriented along the extraordinary axis of the LC cells the LC SLM acts as a phase modulator.[6,8] The face of the LC SLM was imaged onto a camera through a pinhole that passed only the first diffraction orders produced by the LC SLM.

To determine the number of phase levels available and characterize the phase response, we continuously loaded a test image into the LC SLM. The range of pixel values available for the images was [0, 85], which corresponds to a range of approximately 3π in phase. The test image, shown in Fig. 2(a), consisted of eight horizontal bars, the pixel value of each bar being constant, and a border of zero-valued pixels surrounding the collection of bars. The pixel values of the bars increase from the top bar to the bottom bar. The reference surface can be adjusted to produce vertical tilt fringes that are shifted horizontally by different amounts over the area of each bar, where the amount of shift between bars is proportional to the phase difference between those bars. Ideally, the value of each bar can be adjusted until eight uniform shifts between the bars are achieved, thereby determining a set of equally spaced phase levels. During the experiment, two things became apparent: (1) The surface of the device is curved, having curvatures of $\sim\lambda/2$ along the vertical direction and $<\lambda/8$ along the horizontal. (2) The phase response is different for each pixel. So, using the test image shown in Fig. 2(a), we chose pixel values to produce eight uniform average horizontal shifts in the fringe pattern, where each average horizontal shift is a visual average of all the fringe shifts

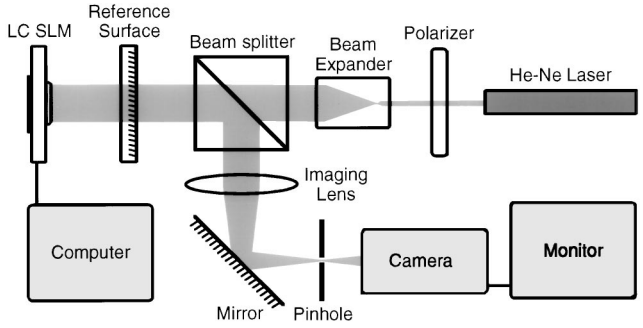

Fig. 1. Fizeau interferometer used to investigate spatial characteristics of the LC SLM.

0146-9592/98/120969-03$15.00/0

Fig. 2. Demonstration of eight phase-level capability: (a) test image loaded to the LC SLM and (b) the theoretical and (c) the measured interferograms produced by the phase image.

between a set of adjacent bars. Table 1 represents a set of eight average phase levels between 0 and 2π. Because only a few pixel values are available between some of these phase levels, it is not possible to have a larger number of equally spaced phase levels with the current device configuration. If we used more bits for each digital-to-analog converter it should be possible to obtain a larger number of phase levels.

Uniform images of the pixel values in Table 1 do not correspond to uniform phase levels because of the device curvature and the variation in the phase response for each pixel. Uniform images of the pixel values in Table 1 were used in the temporal characterization of our device, but corrected phase levels were created for the wave-front-generation experiments. To create the corrected phase levels we assumed that the phase responses of all pixels were identical and were characterized by a fifth-order polynomial, which was least-squares fitted to the average phase levels in Table 1. The corrected phase levels were generated through an iterative process in which the aberration of each phase level was measured and used to generate a set of corrected phase levels. The process started with phase level images of uniform pixel values corresponding to the values in Table 1. After two iterations, all the corrected phase levels were flat to within a deviation of $\lambda/8$. A test image similar to the one shown in Fig. 2(a) was used to ensure that the corrected phase levels were uniformly spaced between 0 and 2π.

We measured the temporal characteristics of the LC SLM by configuring the device as an amplitude modulator.[4] Light from a He–Ne laser, linearly polarized at 45° to the fast axis of the LC cells, was expanded to illuminate the LC SLM through a beam splitter. Reflected light from the LC SLM was focused onto a P–I–N diode by a lens after going back through the beam splitter and an analyzer. The P–I–N diode was connected to a computer, which recorded the intensity of the focused beam. The LC SLM was driven by a square wave of alternating images of uniform pixel values corresponding to a phase value of 0 and an integral multiple of $\pi/4$. In Fig. 3(a) the temporal response to a square-wave input of a period of 98 ms between phase values 0 and $\pi/4$ is shown. When a portion of the response curve was fitted to an exponential function, we found that the rise time, which is the time for the detected intensity to reach 90% of its asymptotic value, was 9 ms and the fall time was 10 ms. Small ripples in the response were observed owing to the ac operation of the device, i.e., toggling between true and inverse frames. The response to a square-wave input of period 390 ms between phase values 0 and $7\pi/4$ is shown in Fig. 3(b). The recorded intensity goes through extrema between the steady-state values as a result of the sinusoidal amplitude modulation.[8] The temporal responses between the phase value 0 and other phase values are summarized in Table 2. We observed that the fall time increases steadily as the phase value increases and that the rise time suddenly increases for the phase value $7\pi/4$, limiting arbitrary phase modulation speed to approximately 4.5 Hz. As expected, this LC SLM is faster than transmissive devices, which have thicker LC cells, as the switching time of the LC SLM is proportional to the square of the LC-layer thickness.[9] It was suggested that combining a dual-frequency LC phase modulator with a transient nematic effect could provide a phase modulation rate of 500 Hz.[4]

To investigate the wave-front-generation capability of the LC SLM we loaded image files of several Zernike polynomials into the LC SLM. The Zernike polynomials were calculated (mod 2π) and quantized by use of the eight corrected phase levels discussed above. Using the LC SLM device in the Fizeau interferometer (see Fig. 1), we recorded interferograms for image files

Table 1. Pixel Values Corresponding to Phase Levels between 0 and 2π

Pixel Value	Phase (rad)
0	0
19	$\pi/4$
32	$\pi/2$
38	$3\pi/4$
43	π
47	$5\pi/4$
51	$3\pi/2$
55	$7\pi/4$
58	2π

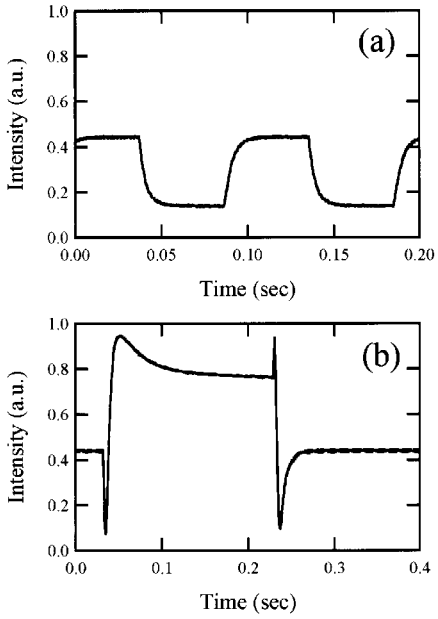

Fig. 3. Temporal response of the LC SLM for a square-wave input between the phase values: (a) 0 and $\pi/4$ with a period of 98 ms, (b) 0 and $7\pi/4$ with a period of 390 ms.

Table 2. Response Times for the LC SLM

Phase (rad)	Rise Time (ms)	Fall Time (ms)
$\pi/4$	9	10
$\pi/2$	19	11
$3\pi/4$	28	15
π	27	16
$5\pi/4$	27	19
$3\pi/2$	19	21
$7\pi/4$	110	24

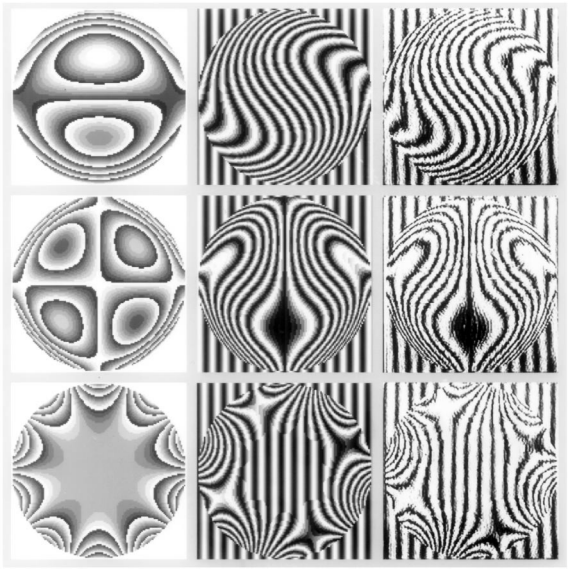

Fig 4. Demonstration of wave-front-generation capability: The first column contains quantized phase images loaded to the LC SLM, and the second and third columns contain a theoretical and a measured interferogram, respectively, corresponding to each phase image. Each row represents a different Zernike polynomial [see Eqs. (1)].

corresponding to various Zernike polynomials. The first 55 Zernike polynomials, up to and including ninth-order terms, $V_9{}^9$, in the notation of Born and Wolf,[10] were loaded into the LC SLM and produced interferograms that were in excellent agreement with theoretical predictions that assumed ideally quantized images. Three of the Zernike polynomials and the corresponding interferograms are presented in Fig. 4. The left-hand column of Fig. 4 contains the image files loaded into the LC SLM, and the second and third columns contain theoretical and measured interferograms, respectively. A different Zernike polynomial is represented in each row of Fig. 4. From the top row to the bottom row, the Zernike polynomials represented are given in units of wavelength by

$$\mathrm{Im}\left\{\sqrt{8}\,V_3{}^1[\rho\sin(\theta),\rho\cos(\theta)]\right\} = \sqrt{8}\,\rho(3\rho^2-2)\sin(\theta),$$

$$\mathrm{Im}\left\{\sqrt{10}\,V_4{}^2[\rho\sin(\theta),\rho\cos(\theta)]\right\} = \sqrt{10}\,\rho^2(4\rho^2-3)\sin(2\theta),$$

$$\mathrm{Im}\left\{\sqrt{12}\,V_5{}^5[\rho\sin(\theta),\rho\cos(\theta)]\right\} = \sqrt{12}\,\rho^5\sin(5\theta), \qquad (1)$$

where the functions $V_n{}^l$ are defined by Born and Wolf[10] and ρ and θ are normalized radial and azimuthal angle coordinates, respectively, for the pupil plane located at the surface of the LC SLM. The Zernike polynomials represented in Eqs. (1) correspond to deviations of 1λ rms and of $\sqrt{32}\,\lambda$, $\sqrt{40}\,\lambda$, or $\sqrt{24}\,\lambda$ peak to peak, respectively. As expected, our 16,384-element device is able to produce Zernike polynomials of significantly larger deviations and higher orders than the previously reported 69-element[2] and 127-element[3] devices.

In conclusion, we have demonstrated that a 128×128 element LC SLM can produce high-quality wave fronts, as demonstrated by wave-front generation of several Zernike polynomials that exceed a maximum peak-to-peak phase variation of 6λ. We determined that only eight equal phase levels between 0 and 2π are available for wave-front generation with the device used in our experiments. This limitation is due to the fact that the drive electronics for the device uses 8-bit digital-to-analog converters. In terms of temporal characteristics, the rate of arbitrary phase modulation for the Boulder Nonlinear Systems LC SLM is limited to approximately 4.5 Hz. Although the reflective LC SLM is faster than a transmissive one because of its smaller LC-cell thickness, it still requires improvement before it can be used for real-time AO applications. However, we note that the current device should be quite useful for AO retinal imaging, for which the capability of high-quality wave-front generation is more important than real-time operation.

The authors are grateful to the staff of Boulder Nonlinear Systems, Inc., for their assistance and to D. R. Williams for many fruitful discussions. This research is supported in part by the New York State Center for Electronic Imaging Systems. D. J. Cho acknowledges financial support from Ajou University.

References

1. U. Efron, *Spatial Light Modulator Technology* (Dekker, New York, 1995).
2. G. D. Love, Appl. Opt. **36,** 1517 (1997).
3. L. Thibos and A. Bradley, Optom. Vis. Sci. **74,** 581 (1997).
4. A. Kudryashov, J. Gonglewski, S. Browne, and R. Highland, Opt. Commun. **141,** 247 (1997).
5. J. Liang, D. R. Williams, and D. T. Miller, J. Opt. Soc. Am. A **14,** 2884 (1997).
6. K. Bauchert, S. Serati, G. Sharp, and D. McKnight, Proc. SPIE **3073,** 170 (1997).
7. Boulder Nonlinear Systems, Inc., 1898 South Flatiron Court, Boulder, Colo. 80301.
8. J. de Bougrenet de la Tocnaye and L. Dupont, Appl. Opt. **36,** 1730 (1997).
9. V. Dorezyuk, A. Naumov, and V. Shmal'gauzen, Sov. Phys. Tech. Phys. **34,** 1389 (1989).
10. M. Born and E. Wolf, *Principles of Optics* (Pergamon, New York, 1989).